Published in final edited form as:
Neuroscience. 2010 December 1; 171(2): 513–523. doi:10.1016/j.neuroscience.2010.08.057.

Changes in and dorsal to the rat suprachiasmatic nucleus during early pregnancy

Jessica A. Schrader[a], **Antonio A. Nunez**[b,c], and **Laura Smale**[a,b,c,*]

Jessica A. Schrader: stjohnj4@msu.edu; Antonio A. Nunez: nunez@msu.edu

[a]Department of Zoology, Michigan State University, East Lansing, Michigan 48824, USA

[b]Department of Psychology, Michigan State University, East Lansing, Michigan 48824, USA

[c]Neuroscience Program, Michigan State Univertisity, East Lansing, Michigan 48824, USA

Abstract

Circadian rhythms in behavior and physiology change as female mammals transition from one reproductive state to another. The mechanisms responsible for this plasticity are poorly understood. The suprachiasmatic nucleus (SCN) of the hypothalamus contains the primary circadian pacemaker in mammals, and a large portion of its efferent projections terminate in the ventral subparaventricular zone (vSPZ), which also plays important roles in rhythm regulation. To determine whether these regions might mediate changes in overt rhythms during early pregnancy, we first compared rhythms in Fos and Per2 protein expression in the SCN and vSPZ of diestrous and early pregnant rats maintained in a 12:12 light/dark cycle. No differences in the Fos rhythm were seen in the SCN core, but in the SCN shell, elevated Fos expression was maintained throughout the light phase in pregnant, but not diestrous, rats. In the vSPZ, the Fos rhythm was bimodal in diestrous rats, but this rhythm was lost in pregnant rats. Peak Per2 expression was phase-advanced by four hours in the SCN of pregnant rats, and some differences in Per2 expression were found in the vSPZ as well. To determine whether differences in Fos expression were due to altered responsivity to light, we next characterized light-induced Fos expression in the SCN and vSPZ of pregnant and diestrous rats in the mid-subjective day and night. We found that the SCN core of the two groups responded in the same way at each time of day, whereas the rhythm of Fos responsivity in the SCN shell and vSPZ differed between diestrous and pregnant rats. These results indicate that the SCN and vSPZ are functionally re-organized during early pregnancy, particularly in how they respond to the photic environment. These changes may contribute to changes in overt behavioral and physiological rhythms that occur at this time.

Keywords

Circadian rhythm; ventral subparaventricular zone; Fos; Per2; diestrous; reproduction

Circadian rhythms have a period of roughly 24 hours and are generated endogenously. When synchronized to the external environment, these rhythms allow organisms to anticipate predictable daily fluctuations in the environment and appropriately time behavioral and

*Correspondance to: Laura Smale, 108 Giltner Hall, Michigan State University, East Lansing, MI 48824, USA, Tel: (517) 432-1632, Fax: (517) 353-1652, smale@msu.edu.

physiological events in relation to those changes (Moore-Ede et al., 1982). The circadian timekeeping system plays an important role in the coordination of a variety of physiological and behavioral processes essential for mammalian reproduction. In some mammals, including many rodents, the timing of ovulation is regulated by this system (for review, see de la Iglesia and Schwartz, 2006), and rhythms in mating behavior have been observed in multiple species (Beach and Levinson, 1949; Dobson and Michener, 1995; Gilbert et al., 1985; Hansen et al., 1979; Harlan et al., 1980; Mahoney and Smale, 2005). This probably optimizes the likelihood of successful fertilization. However, in all therian mammals, fertilization is followed by gestation (pregnancy) and lactation. Circadian rhythms play important roles during these reproductive states as well, although significantly less work has focused on this issue.

The best-characterized animal model of circadian processes operating during pregnancy is the nocturnal lab rat. During early pregnancy in this species, locomotor activity generally decreases and becomes less rhythmic (Rosenwasser et al., 1987), whereas body temperature rhythms show an advance in their rising phase and a reduction in amplitude attributable to increases in the daily temperature minimum (Kittrell and Satinoff, 1988). Sleep patterns are altered, and the total amount of time spent in both non-rapid eye movement sleep (NREMS) and rapid eye movement sleep (REMS) during the dark phase increases during early pregnancy, as does the number of REMS bouts in the dark phase (Kimura et al., 1996). Rhythms in hormone secretion also change during early pregnancy in the rat. Those of circulating adrenal corticotropin hormone (ACTH) and corticosterone experience decreases in amplitude due to a reduction in the peak values, and the rising phase of the rhythm in ACTH is also advanced (Atkinson and Waddell, 1995). Additionally, a prolactin rhythm, with peaks around dawn and dusk, emerges in early pregnancy and promotes progesterone secretion by the corpora lutea (Butcher et al., 1972; Freeman et al., 2000). While these changes have been known for some time, the neural mechanisms responsible for changes in all but the prolactin rhythm have received scant attention.

The neural mechanisms controlling circadian rhythms in mammals have been well-characterized in males and nulliparous females, and it is firmly established that the suprachiasmatic nucleus (SCN), located bilaterally in the anterior hypothalamus, houses the primary pacemaker that generates these rhythms (Moore and Eichler, 1972; Ralph et al., 1990; Rusak, 1977; Stephan and Zucker, 1972). The SCN is functionally and neurochemically heterogeneous, and it may be divided into two main subregions, referred to by some as the “core” and the “shell” and by others as the ventrolateral (vl-) and dorsomedial (dm-) SCN (Morin, 2007). Here, we use the terms core and shell (as in Moore et al., 2002), even when referring to reports in which the authors used the terms vl-SCN and dm-SCN, to differentiate between the two subregions (e.g. Lee et al., 1998).

The pacemaker of the SCN entrains to the light/dark (LD) cycle via innervation of the SCN core by the retinohypothalamic tract (Johnson et al., 1988; Levine et al., 1991; Moore and Lenn, 1972; Moore et al., 2002). This region also receives non-photic input, and it conveys the two kinds of information to the SCN shell, which also receives non-photic inputs from other brain regions (Antle and Silver, 2005; Daikoku et al., 1992; Ibata et al., 1993; Ibata et al., 1997; Moore et al., 2002). The SCN shell integrates these inputs with endogenous circadian processes and serves primarily as an SCN output subregion (Moore et al., 2002). Its major target is the subparaventricular zone (SPZ; Leak and Moore, 2001; Watts and Swanson, 1987; Watts et al., 1987; Watts, 1991), which projects to many of the same targets as the SCN and may integrate circadian signals and homeostatic drive (Abrahamson and Moore, 2006; Kriegsfeld et al., 2004; Lu et al., 2001; Morin et al., 1994; Saper et al., 2005; Schwartz et al., 2004; Watts and Swanson, 1987; Watts et al., 1987). The ventral region of the SPZ (vSPZ), lies immediately dorsal to the SCN shell and is important in the control of locomotor activity rhythms (Abrahamson and Moore, 2006; Lu et al., 2001; Schwartz et al., 2009).

Although cells in both the core and shell of the rat SCN express the inhibitory neurotransmitter, GABA (Moore and Speh, 1993), the two subdivisions differ with respect to other peptides and transmitters they contain. Cells in the SCN shell primarily express arginine vasopressin (AVP), whereas the primary core output signals are vasoactive intestinal polypeptide (VIP) and gastrin-releasing peptide (GRP; Antle and Silver, 2005; Moore et al., 2002; Romijn et al., 1998). VIP and GRP neurons in the rat SCN core innervate the entire SCN and also project beyond the nucleus (Daikoku et al., 1992; Ibata et al., 1993; Ibata et al., 1997; Moore et al., 2002). Both subregions contain oscillator cells, which each have a molecular transcription/translation loop that takes roughly 24 hours to complete. This "molecular oscillator" involves a transcription-translation feedback loop comprised of multiple "clock" genes and their protein products. These include the period (Per) proteins, which rhythmically influence the transcription of other genes, referred to as clock-controlled genes (Bell-Pedersen et al., 2005; Dunlap, 1999; Reppert and Weaver, 2002). Cells expressing this feedback loop are more prevalent in the SCN shell, where they co-express AVP, but some are in the core and co-express VIP (Dardente et al., 2002). Other populations of cells, called extra-SCN oscillators, express the same transcription-translation feedback loop as that within the SCN. These populations have been found within the brain and throughout the periphery and, together with the SCN, comprise the circadian system (Guilding and Piggins, 2007; Hastings et al., 2003; Reppert and Weaver, 2002; Weinert, 2005).

The various changes in rhythms that occur during early pregnancy raise the question of whether and how the circadian timekeeping system might be involved in promoting them. One possibility is that the SCN is the driving force behind these changes. If so, changes in SCN rhythms in peptide expression, clock gene oscillations, and/or neuronal firing should be apparent during this phase of reproduction. Alternatively, the SCN might remain the same, while extra-SCN oscillators and/or non-circadian systems are altered, perhaps in a site-specific manner. The purpose of this study was to examine the possibility that rhythms in the SCN, and its primary target, the vSPZ, differ between non-pregnant and early pregnant rats. To do this, we characterized rhythms in Per2, a key component of the molecular oscillator, and Fos, the protein product of the immediate early gene *cfos* that often rises after neuronal activation (Kovacs, 2008), in pregnant and non-pregnant rats. The first group was examined on day 6 of pregnancy, as the changes in overt rhythms described above are all established by that time. Although Per2 expression in the SCN does not appear to vary throughout the estrous cycle (Perrin et al., 2006), estrogens do influence rhythmic and light-induced expression of Fos in the SCN of female rats (Abizaid et al., 2004; Peterfi et al., 2004). Additionally, wheel running activity rhythms are known to vary throughout the estrous cycle in an estrogen-dependent manner in this species (Albers, 1981; Albers et al., 1981; Gerall et al., 1973; Thomas and Armstrong, 1989). Therefore, we selected females on day 1 of diestrus, when circulating gonadal hormones are lowest, for our non-pregnant controls.

The initial experiment revealed differences in Fos expression in the SCN shell and vSPZ between the two groups of females in the mid-light and/or mid-dark phases of the LD cycle. We therefore conducted a second experiment to determine whether rhythms in light-induced Fos expression in the SCN and vSPZ could account for these patterns.

Experimental Procedures

Animals

Animals were adult female and male Sprague-Dawley laboratory rats obtained from Harlan Laboratories (Indianapolis, IN, USA). Males were housed in pairs or groups of three when not paired with females. Females were housed in groups of three or four for a habituation period of at least two weeks and were then single-housed. All subjects were housed in polypropylene cages (48×27×20 cm) with *ad libitum* access to food (Teklad 8640 rodent diet, Harlan) and

water under a 12h:12h light/dark (LD) cycle (unless otherwise noted) with lights on at Zeitgeber Time (ZT) 0 and off at ZT 12. A dim red light (<5 lux) remained on constantly for animal care purposes. All experiments were performed in compliance with guidelines established by the Michigan State University Institutional Animal Care and Use Committee and the National Institutes of Health Guide for the Care and Use of Laboratory Animals. All efforts were made to keep the number of animals used and their discomfort at a minimum.

Determination of estrous cycle stages

Once singly housed, females were subjected to daily vaginal smears with sterile saline-soaked cotton-tipped applicators between ZT 0 and ZT 3 to track their estrous cycles. Applicators were immediately rolled onto glass slides, which were dried and stained with methylene blue dye before examination under a light microscope. Estrous cycle stage was determined as follows: proestrus: predominantly nucleated epithelial cells; estrus: predominantly to exclusively cornified epithelial cells; diestrus (between 2 to 3 consecutive days): predominantly leukocytes, some cornified and/or nucleated epithelial cells and mucus present. At least three estrous cycles were established for each female prior to further experimental manipulations.

Tissue collection and immunocytochemistry

At the time of perfusion, animals were given an overdose of sodium pentobarbital and perfused transcardially with 0.01 M phosphate-buffered saline (PBS), pH 7.2, followed by 4% paraformaldehyde (Sigma, St. Louis, MO) in 0.1 M phosphate buffer. In Experiment 1, 1.3% lysine and 4% sodium periodate were added to the 4% paraformaldehyde. Animals perfused during the dark phase or under constant darkness were fitted with a light-tight hood prior to perfusion to prevent acute exposure to light. Brains were post-fixed for 4 hours, transferred to 20% sucrose solution overnight, and stored in cryoprotectant at 4 °C overnight then at -20 °C until sectioning. Brains were sectioned coronally at 30 μm into three alternate series using either a freezing microtome or cryostat, and sections were placed in cryoprotectant for further storage at -20 °C.

For tissue series that were processed for immunocytochemical staining to detect Fos protein expression in the cell nucleus, free floating sections were rinsed in 0.01 M PBS and then incubated in 5% normal goat serum (NGS; Vector Laboratories, Burlingame, CA, USA) in PBS with 0.3% Triton X-100 (TX) for 1 h at room temperature. After a 10 minute rinse in PBS, sections were incubated with a primary anti-cFos antibody (made in rabbit, Santa Cruz Biochemistry, Santa Cruz, CA, USA; 1:25,000, unless otherwise noted) in 3% NGS and 0.3% TX in PBS on a rotator at 4°C for 48h, unless otherwise noted. Sections were then rinsed in PBS and incubated with a biotinylated secondary goat-anti-rabbit antibody (Vector; 1:200) in 3% NGS and 0.3% TX in PBS for 1 h at room temperature, rinsed again, and then incubated with an avidin-biotin peroxidase complex (0.9% each avidin and biotin solutions; ABC Vectastain kit; Vector) in 0.3% TX with PBS for 1 h at room temperature. Next, sections were rinsed in 0.125 M acetate buffer, pH 7.2, then reacted with diaminobenzidine (DAB; 0.25 mg/mL, Sigma), nickel sulfate (25 mg/mL, Sigma), and hydrogen peroxide (0.825 μL 0.3% H_2O_2 /mL buffer) to yield a blue-black reaction product.

For tissue processed for Per2-immunoreactivity, the tissue was processed in the same manner as for Fos except with a primary anti-Per2 antibody (mPER2 # 38, made in rabbit, 1:5,000, 24 h incubation; a generous gift from Dr. David Weaver, University of Massachusetts, MA, USA). After the reaction for Per2 staining, the tissue was then labeled for detection of tyrosine hydroxylase (TH) for use in another study via the protocol described in Ramanathan et al. (2008).

Some sections were stained for arginine vasopressin (AVP) in order to identify the boundary between the shell and core; these sections initially underwent processing for Fos, as described above, but that reaction failed due to a dilution error. Sections were then processed in the same manner as for Fos with the following exceptions: (1) with a primary anti-vasopressin antibody (made in guinea pig, Peninsula Laboratories, Belmont, CA, USA; 1:30,000; 24 h incubation); (2) with a secondary goat-anti-guinea pig antibody (Vector; 1:200); and (3) after incubation with the avidin-biotin peroxidase complex, the tissue was rinsed in Trizma buffer (pH 7.2, Sigma) then reacted with DAB (0.2 mg/mL, Sigma) and hydrogen peroxide (0.35 μL 30% H_2O_2 /mL buffer) to yield a brown reaction product. All sections were mounted on clean slides, dehydrated, and coverslipped.

Experiment 1: Fos and Per2 rhythms in LD

Here we examined temporal patterns of Fos and Per2 immunoreactivity in both diestrous and pregnant rats. Animals were acclimated for at least two weeks to a 12h:12h LD cycle. Females were then singly housed, and daily vaginal smears were taken. Animals were perfused at 4 h intervals (ZT 2, 6, 10, 14, 18, and 22) either on day one of diestrus or on day 6 of pregnancy. The pregnant females were obtained by placing a male in each female's cage on the morning of proestrus (between ZT 0 and 3). Males were removed the next morning, and a vaginal smear was taken from the female to check for the presence of sperm. If none were detected, the female was re-paired on the morning of her next proestrus period. Once mating had been verified, vaginal smears were discontinued, and the day of confirmation was designated as day 0 of pregnancy. Six days later, pregnancy was confirmed by visual inspection of the uterus at the time of perfusion. One series of brain sections from these animals was processed for detection of Fos, and another was processed for detection of Per2.

Photographs of the SCN/vSPZ were taken from three sections, bilaterally, for each tissue series using a CCD video camera (CX900, MBF Bioscience, Williston, VT, USA) attached to a light microscope (Zeiss, Göttingen, Germany). These images were processed using Adobe Photoshop 7 and imported to Adobe Illustrator CS 4 (Adobe Systems, Mountain View, CA, USA) to draw boundaries for the SCN core and shell and the vSPZ. The borders of the SCN core and shell were based upon the distribution of AVP in the rat SCN (Moore et al., 2002). The vSPZ was sampled by counting cells within a 215 μm × 160 μm rectangle placed immediately dorsal to the SCN and lateral to the third ventricle (Fig. 1). Cells expressing Fos or Per2 were then counted bilaterally in these three regions for all three sections using the NIH ImageJ program (NIH, Bethesda, MD, USA). All counts were made by an investigator unaware of the reproductive state or time of perfusion of each animal.

Experiment 2: Light-induced Fos expression

Animals were acclimated for three weeks to a 12h:12h LD cycle with ZT 0 (lights on) at 1300 h. The females were then singly housed, divided into one of two experimental groups, and subjected to daily vaginal smears to determine the estrous cycle of each individual. Rats in the first group (diestrous) were moved to a separate room in constant darkness (DD) on the morning of proestrus (between ZT 0 and 3). Daily vaginal smears were taken from them in DD to ensure that they were still cycling. On the first day of diestrus (two days after entering DD), experimental females were transferred to a separate room for 30 min in DD and subsequently exposed to a one hour light pulse (250 lux) beginning at either circadian time (CT) 5 or CT 17. Animals were perfused immediately after the light pulse ended at CT 6 or CT 18 (the equivalents of the ZTs from the previous LD cycle). In the second group, females were mated and their pregnancies confirmed as in Experiment 1. Once mating had been verified, vaginal smears were discontinued, and the day of confirmation was designated as day 0 of pregnancy. Four days later, females were moved to DD, as above, and, after two days (i.e. day 6 of pregnancy), they were subjected to the same light pulse/perfusion paradigm as females in the

diestrous group. For both the pregnant and diestrous groups, control females were subjected to the same treatments but did not experience a light pulse in the hour prior to perfusion.

Sections from one series of tissue were processed for Fos immunoreactivity (Fos primary concentration of 1:5,000; incubated for 24 h). We counted the number of Fos-positive cells in the SCN core, SCN shell, and vSPZ bilaterally in each section with a light microscope equipped with a drawing tube (Leitz, Laborlux S, Wetzlar, Germany). The borders of the SCN core and shell were based upon the distribution of AVP in adjacent sections, and the vSPZ was sampled as described above (Fig. 1). All counts were made by an investigator unaware of the reproductive state, time of perfusion, or light treatment of each animal.

Quantitative and Statistical Analysis

In each experiment, three sections (one rostral, middle, and caudal) through the SCN and vSPZ were selected from each animal for analysis. For each region of interest (SCN core, SCN shell, and vSPZ), counts of labeled cells from all sections within each individual were summed. Each sum was then divided by the value from the individual with the highest number of immunoreactive cells in that region to produce a percentage of maximum expression value for each individual. For all figures, these percentages, without further transformation, are presented as means ± standard errors (SE).

The data for expression of each protein in each region were subjected to Levene's test for homogeneity of variances; if they did not meet the criteria of this test, the data were then arcsine-transformed. If arcsine transformation did not equalize the variances, then nonparametric tests (detailed below) were used to analyze the original percent of maximum values for that region/protein combination. All data analyses were conducted with SPSS 17 software (SPSS Inc., Chicago, IL, USA). All differences were considered significant when $P<0.05$, except in cases where Bonferroni corrections were required (see below). Statistical details are omitted from the text when they are presented in figure legends.

Experiment 1—A total of 57 females were used in the final analysis (n=28 diestrous, n=29 pregnant, n=4-6 per time point for each reproductive state). For data that met the homogeneity of variance criteria, 2-way analyses of variance (ANOVAs) were performed, with reproductive state (pregnant or diestrous) and time of perfusion (ZT) as between-subjects factors. Relevant post-hoc least significant difference (LSD) tests were conducted with these data when any significant interactions were found. Data from the SCN core and Per2 expression data from the vSPZ were arcsine-transformed prior to these analyses. For data that did not meet the homogeneity of variance criteria even when transformed, nonparametric analyses were conducted to compare ZTs within each reproductive state (Kruskal-Wallis tests, followed by post-hoc pairwise Mann-Whitney U tests when significant effects were found). We also compared reproductive states at each ZT where the standard errors of the pregnant and diestrous groups did not overlap (SCN shell Fos: ZT 6, 10, and 14; shell Per2: ZT 14 and 22; Mann-Whitney U tests). Bonferroni corrections were applied to these pairwise tests such that statistical significance was set at $P<0.017$ for Fos in the shell and at $P<0.025$ for Per2 in the shell.

Experiment 2—A total of 47 females were used in the final analysis (n=23 diestrous, n=24 pregnant, n=5-7 per light treatment/CT for diestrous rats and n=6 per light treatment/CT for pregnant rats). For data that met the homogeneity of variance criteria, a 3-way ANOVA was performed, with reproductive state (pregnant or diestrous), time of perfusion (CT), and light treatment (pulse or control) as between-subjects factors. Relevant post-hoc LSD tests were conducted with these data when any significant interactions were found. Data from the SCN core and shell did not meet the homogeneity of variance criteria even when transformed, and

nonparametric analyses were conducted to compare the effects of light pulses (pregnant and diestrous separately) at each CT (Mann-Whitney U tests). Post-hoc examination of the data in these two subregions led us to also compare the effects of a light pulse on Fos expression in the SCN core between CT 6 and CT 18 (reproductive states combined) as well as the effect of a light pulse on Fos expression in the shell at CT 18 between pregnant and diestrous rats (Mann-Whitney U tests). For each SCN subregion, we therefore applied a Bonferroni correction of $P<0.01$ for statistical significance (5 tests/subregion).

Results

Experiment 1

SCN core—Representative photomicrographs depicting patterns of Fos and Per2 expression are shown in Fig. 2. In the core, a two-way ANOVA of the Fos expression data revealed a significant main effect of ZT, with peak expression at ZT 2 (Fig. 3A; $F=27.034$, $df=5$, $P<0.001$). We also found a trend towards significance for higher Fos expression in pregnant than diestrous females ($F=3.623$, $df=1$, $P<0.065$), and there was no interaction between reproductive state and ZT ($F=0.808$, $df=5$, $P>0.5$). In the core, a two-way ANOVA of the Per2 expression data revealed a significant interaction between reproductive state and ZT ($F=3.316$, $df=5$, $P<0.02$). In diestrous females, the peak of the Per2 rhythm was narrow and occurred at ZT 18 (Fig. 3B; simple main effect of ZT: $F=6.171$, $df=5$, $P<0.001$). However, in pregnant rats, the peak of the Per2 rhythm was slightly broader (simple main effect of ZT: $F=2.644$, $df=5$, $P<0.05$), and expression was highest at ZT 14, at which time there was significantly more Per2 expression in pregnant than diestrous females.

SCN shell—As in the core, Fos expression in the SCN shell peaked at ZT 2 and dropped to basal levels from ZT 6 through ZT 22 in the diestrous females (Fig. 3C; significant effect of ZT: $X^2=11.918$, $df=5$, $P<0.04$, Kruskal-Wallis test). In pregnant rats, however, expression remained high throughout the light phase and did not reach significantly lower levels from ZT 2 or 6 until ZT 18 (significant effect of ZT: $X^2=13.791$, $df=5$, $P<0.02$, Kruskal-Wallis test). At ZT 6, expression was also significantly higher in pregnant than diestrous rats. Also similar to the core, the rhythm of Per2 expression in the SCN shell of diestrous rats peaked at ZT 18 (Fig. 3D; significant effect of ZT: $X^2=13.372$, $df=5$, $P\leq0.02$, Kruskal-Wallis test), but the rhythm in pregnant females was of a lower amplitude with a broader peak from ZT 10 to ZT 18 (significant effect of ZT: $X^2=12.420$, $df=5$, $P<0.03$, Kruskal-Wallis test). There was a trend towards significance for higher expression in the shell of pregnant rats than in that of diestrous females at ZT 14 ($U=1$, $P<0.035$, Mann-Whitney U test). Although interactions cannot be directly assessed with nonparametric tests, these patterns suggest that an interaction between reproductive state and ZT may exist for both Fos and Per2 expression in the SCN shell.

vSPZ—A two-way ANOVA of the Fos expression data in the vSPZ revealed a significant interaction between reproductive state and ZT ($F=3.459$, $df=5$, $P<0.02$). In diestrous rats, there was a bimodal rhythm in Fos expression in the vSPZ, with peaks at ZT 2 and ZT 18 (Fig. 3E; simple main effect of ZT: $F=8.811$, $df=5$, $P<0.001$), but no rhythm existed in the vSPZ of pregnant rats (simple main effect of ZT: $F=1.724$, $df=5$, $P>0.15$). Expression in the vSPZ of the two groups differed at ZT 6 (more in pregnant females) and at ZT 18 (more in diestrous females). A two-way ANOVA of the Per2 expression data in the vSPZ revealed a significant interaction between reproductive state and ZT ($F=2.822$, $df=5$, $P<0.03$). There was no significant rhythm in Per2 expression in the vSPZ in either diestrous or pregnant rats (Fig. 3F; simple main effects of ZT: diestrous: $F=2.191$, $df=5$, $P<0.095$; pregnant: $F=0.932$, $df=5$, $P>0.4$). However, in the diestrous group, most of the Per2 immunoreactivity was detected in animals perfused at ZT 18 and 22, when Per2 expression was low in pregnant females. Expression

significantly differed between the two reproductive states only at ZT 14, as pregnant females again had higher Per2 expression than diestrous females at this time.

Experiment 2

SCN core—Representative photomicrographs depicting patterns of light-induced Fos expression are shown in Fig. 4. Light-induced Fos expression was similar in the SCN core of pregnant and diestrous rats, which expressed more Fos in the core than controls at both CT 6 and CT 18, with significantly more light-induced expression evident at CT 18 than at CT 6 (Fig. 5A; U=20.5, P<0.005, Mann-Whitney U test). Although we could not directly test interactions with nonparametric tests, these data suggest that neither light treatment nor time of perfusion interacted with reproductive state, although they did appear to interact with one another.

SCN shell—A light pulse at CT 6 appeared to increase Fos in the SCN shell of diestrous females, but this change did not reach significance after the Bonferroni correction (Fig. 5B; U=6, P<0.04, Mann-Whitney U test). This was not the case in pregnant rats, in which there was clearly no effect of the light pulse on Fos expression in the shell (U=17, P>0.9, Mann-Whitney U test). At CT 18, however, a light pulse led to higher Fos expression in both groups of rats. Pregnant females appeared to express more Fos in the shell than diestrous females after a light pulse at this time, but this difference did not reach significance (U=5.5, P<0.085, Mann-Whitney U test). Although we could not directly test interactions with nonparametric tests, these data suggest that a three-way reproductive state × light treatment × CT interaction may exist.

vSPZ—A three-way ANOVA of the Fos expression data revealed a significant three-way interaction (reproductive state × light treatment × CT, F=4.374, df=1, P<0.05). Diestrous and pregnant rats exhibited strong responses to light at opposite times of day, with light-pulsed diestrous females expressing more Fos in the vSPZ than controls at CT 6 and light-pulsed pregnant rats expressing more Fos in the vSPZ than controls at CT 18 (Fig. 5C).

Discussion

The results of these two studies reveal fundamental changes in oscillatory processes within the SCN and vSPZ. It is unclear whether the expression patterns of Fos and Per2 in these regions change in relation to those of other proteins, such as output signals or other clock proteins not examined here, or if the entire functional oscillator and output machinery are changing together. Nonetheless, altered patterns in Fos expression most likely reflect altered functioning within the SCN and vSPZ, and the shifts in Per2 expression profiles demonstrate that the molecular oscillator is not functioning in the same manner in diestrous and early pregnant rats, regardless of whether other clock proteins are shifting with Per2. The changes reported here demonstrate that processes within the SCN and vSPZ are sensitive to shifts in reproductive state and may potentially be involved in driving alterations in physiological and behavioral rhythms in early pregnancy.

An unexpected result from this study was the discovery of a potential sex difference in how the SCN responds to light in this species. Although male rats have repeatedly shown strong induction of Fos expression after a light pulse in the subjective night, it has long been thought that the SCN is non-responsive during the subjective day (Edelstein et al., 2000; Guido et al., 1999; Rusak et al., 1990; Schwartz et al., 1994; Schwartz et al., 2000). However, both diestrous and pregnant rats expressed more Fos in the SCN core after a light pulse at CT 6, and the shell also appeared responsive in the diestrous rats at this time. Further studies should be conducted

to confirm whether this is a true sex difference and whether it is reliant upon gonadal sex hormones.

The SCN core

Expression of Fos in the SCN core did not differ between pregnant and diestrous rats (Fig. 3A). In both groups, Fos peaked at ZT 2 and returned to baseline levels by ZT 6, a pattern that mirrors those reported previously in male rats (Guido et al., 1999;Jac et al., 2000;Schwartz et al., 2004;Schwartz et al., 1994;Sumova et al., 2000;Sumova and Illnerova, 2005). It is likely that the peak at ZT 2 reflects the induction of Fos by lights-on (Schwartz et al., 1994). Light-induced Fos expression in the SCN core, which occurred at both CT 6 and CT 18 but was higher at CT 18, was also similar in pregnant and diestrous rats (Fig. 5A).

In contrast to Fos, Per2 in this region did vary as a function of reproductive state (Fig. 3B). In diestrous rats, Per2 peaked at ZT 18 and dropped by ZT 22, whereas the peak occurred four hours earlier in pregnant rats. The new temporal relationship between Fos and Per2 rhythms might reflect either changes in phase relationships amongst various oscillatory processes within cells or changes in functionally distinct populations of cells within the SCN core (Antle and Silver, 2005;Moore et al., 2002;Romijn et al., 1998). Either way, transcriptional pathways driving Fos and Per2 expression in the core appear to be differentially affected by stimuli associated with mating, fertilization, or early pregnancy.

The SCN shell

In the SCN shell of diestrous animals kept in an LD cycle, the rhythm of Fos expression mirrored that in the core, with Fos rising sharply from ZT 22 to ZT 2 and then dropping by ZT 6 (Fig. 3C). In pregnant rats, the rising phase of the rhythm was the same, but high levels were maintained throughout the light phase. This was unlikely due to an increase in responsivity to photic cues, as light did not induce Fos expression in the SCN shell of pregnant rats in the mid-subjective day in DD (Fig. 5B). At CT 18, there appeared to be a higher Fos response to light in the SCN shell in pregnant females than in diestrous ones (Fig. 5B), but this difference was not statistically significant.

As was the case in the core, the peak in the rhythm of Per2 expression in the shell was phase-advanced during early pregnancy (Fig. 3D). In pregnant rats the interval of elevated Per2 in the shell, like that of Fos, also appeared to be broader than in the shell of diestrous females. These patterns raise the possibility that the mechanisms responsible for the pregnancy-induced changes in Per2 and Fos expression in the shell are linked. This region of the SCN is less heterogeneous in cell phenotype than the core, so perhaps Fos and Per2 are more often expressed in the same cells, such as those containing AVP (Dardente et al., 2002). The present data raise the possibility that rhythms in AVP expression might change in early pregnancy, which could contribute to some of the changes in behavior and physiology that occur in this reproductive state.

The SCN core vs. shell

The difference between the SCN core and shell with respect to the plasticity of their rhythms in Fos expression during early pregnancy is intriguing. Specifically, whereas the transition from diestrus to early pregnancy was associated with changes in Fos rhythms in the shell but not the core in the current study (Fig. 3), Lee et al. (1998) found that the transition from early to late pregnancy was associated with changes in the core but not the shell. Rhythms in the core during early pregnancy were somewhat different in these two studies because animals were not sampled around the peak in the early light phase in the Lee et al. study (1998). Overall, however, the data from their study and ours indicate that changes in Fos expression in the shell during early pregnancy are maintained in late pregnancy, whereas the Fos rhythm in the core

does not change until the transition from early to late pregnancy. Thus, Fos expression appears to change in different ways in these two compartments of the SCN as pregnancy progresses.

Whereas pregnancy influenced patterns of Fos expression in different ways in the SCN core and shell, its effect on the peaks of Per2 rhythms in these two regions was the same. The concordance with respect to Per2 expression raises the possibility that altered oscillations in clock gene expression in the two regions of the SCN might be interdependent and may play a role in the mediation of changes in behavioral and physiological rhythms during early pregnancy.

Changes in the vSPZ during early pregnancy

Fos expression in the vSPZ was quite different in diestrous and pregnant females (Fig. 3E). In diestrous rats, a clear bimodal rhythm was evident, with peaks at ZT 2 and again at ZT 18. This pattern differs from that seen in the SCN shell in these animals, confirming that the vSPZ is not a simple functional extension of the shell. Interestingly, the second peak was lost during early pregnancy, whereas the first was extended, lasting from ZT 2 through ZT 6. The vSPZ of laboratory rats has not been thoroughly described, but, in males, there is a unimodal, light-dependent Fos rhythm in this region that is very similar to that seen here in pregnant females (Schwartz et al., 2004). The rhythm disappears when males are housed in DD, suggesting that the peak at ZT 1 is stimulated by light onset (Schwartz et al., 2004). This is also likely to be the case for the peak at ZT 2 in both groups of females in the current study. The second peak, at ZT 18 in diestrous females, has not been reported previously in male rats and is more puzzling. Although its functional implications are not obvious, these patterns reveal a form of plasticity, and a sex difference, in the region that has not been seen before.

Under DD conditions, there were no effects of ZT on Fos expression in the vSPZ in either group of females (Fig. 5C). However, in diestrous females, a light pulse induced Fos in the vSPZ at CT 6 but not CT 18, whereas in pregnant females, the opposite pattern was observed. Intriguingly, this parallels the differences in Fos expression at ZT 6 and ZT 18 in an LD cycle (Fig. 3E), in that rats of both groups exhibited a response to light at a time when Fos was low at the corresponding time in LD. In DD, however, no variation due to time of day or reproductive state was apparent in the absence of a light pulse (Fig. 5C). This suggests that the Fos rhythms seen in the vSPZ of both pregnant and diestrous rats kept on an LD cycle may not be endogenous, as is the case for males (Schwartz et al., 2004). However, the patterns of response to light pulses suggest that an endogenous rhythm in responsiveness to light may exist in the vSPZ and that this rhythm is very different in pregnant and diestrous females. As no significant rhythm in Per2 was found in the vSPZ of either pregnant or diestrous rats, it is likely that rhythms in Fos responses to light in the vSPZ are driven by inputs from the SCN or retina in these animals.

The role of the SCN and vSPZ during early pregnancy

The changes in Fos and Per2 rhythms seen in this study may contribute to changes in physiological and behavioral rhythms that occur during this critical phase of pregnancy. This is supported by some comparisons between patterns seen in our data and those from previous reports of rhythms in early pregnancy. For example, the vSPZ is necessary for the generation of activity rhythms in rats (Abrahamson and Moore, 2006; Lu et al., 2001). During early pregnancy, when locomotor rhythms are lost in DD (Rosenwasser et al., 1987), neither Fos nor Per2 expression in the vSPZ were rhythmic (Fig. 3). This is especially intriguing because core body temperature, which is normally correlated with activity (Refinetti, 1997; Refinetti, 1999), remains robustly rhythmic (Kittrell and Satinoff, 1988). The loss of Fos and Per2 rhythms in the vSPZ might therefore contribute to a dissociation between daily patterns of body

temperature and activity, and perhaps even a loss of locomotor activity rhythms, during early pregnancy.

We also found phase advances in Per2 expression in the SCN, which correlate in magnitude with the advance of the peak of the core body temperature rhythm (Kittrell and Satinoff, 1988). Similarly, the peaks of circulating ACTH and corticosterone rhythms are lowered (Atkinson and Waddell, 1995), as is the peak of Per2 expression in the SCN shell. Although there are no immediately apparent direct correlations between patterns seen in our data and the emergence of bimodal rhythms in prolactin or in the increase in nighttime sleep (Butcher et al., 1972; Kimura et al., 1996), it is still possible that the changes we observed contribute to these effects.

One important question raised by our results is how the changes in Fos and Per2 expression in the core, shell, and vSPZ associated with pregnancy are related to each other. One possibility is that the advance in phase of the Per2 rhythm in the core leads to changes in signals that it sends to the shell and to the vSPZ, where input from the core and shell converge (Antle and Silver, 2005; Daikoku et al., 1992; Ibata et al., 1993; Ibata et al., 1997; Leak and Moore, 2001; Moore et al., 2002; Watts and Swanson, 1987; Watts et al., 1987; Watts, 1991). This model would suggest that a modification in how the core influences the shell and vSPZ contributes to the suite of changes in rhythms that emerge during pregnancy. However, other components of the circadian system, either within or downstream from the SCN and vSPZ, as well as regulatory networks outside of the circadian system altogether, are almost certainly involved as well. Further examination of how these systems change will be necessary to determine how overt rhythms are altered during early pregnancy.

Acknowledgments

We thank Erin Walaszczyk, Tara Kisnonsky, Anthony Yuhas, Nick Graff, Elissa Pastuzyn, Molly Skaer, Adam Stowie, Alexandra Castillo-Ruiz, Anna Baumgras, and Dr. Chidambaram Ramanathan for technical assistance; Ray Figueira, Dr. Lily Yan, Dr. Theresa Lee, Dr. Kay Holekamp, and Dr. Sharleen Sakai for technical and/or statistical advice; and Dr. David Weaver for providing the Per2 antibody. This work was supported by a NIH grant (RO1 MH53433) to L.S.

References

Abizaid A, Mezei G, Horvath TL. Estradiol enhances light-induced expression of transcription factors in the SCN. Brain Res 2004;1010:35–44. [PubMed: 15126115]

Abrahamson EE, Moore RY. Lesions of suprachiasmatic nucleus efferents selectively affect rest-activity rhythm. Mol Cell Endocrinol 2006;252:46–56. [PubMed: 16793198]

Albers HE. Gonadal hormones organize and modulate the circadian system of the rat. Am J Physiol Regul Integr Comp Physiol 1981;241:62–66.

Albers HE, Gerall AA, Axelson JF. Effect of reproductive state on circadian periodicity in the rat. Physiol Behav 1981;26:21–25. [PubMed: 7195042]

Antle MC, Silver R. Orchestrating time: arrangements of the brain circadian clock. Trends Neurosci 2005;28:145–151. [PubMed: 15749168]

Atkinson HC, Waddell BJ. The hypothalamic-pituitary-adrenal axis in rat pregnancy and lactation: circadian variation and interrelationship of plasma adrenocorticotropin and corticosterone. Endocrinology 1995;136:512–520. [PubMed: 7835284]

Beach FA, Levinson G. Diurnal variations in the mating behavior of male rats. Proc Soc Exp Biol Med 1949;72:78–80. [PubMed: 15391680]

Bell-Pedersen D, Cassone VM, Earnest DJ, Golden SS, Hardin PE, Thomas TL, Zoran MJ. Circadian rhythms from multiple oscillators: lessons from diverse organisms. Nat Rev Genet 2005;6:544–556. [PubMed: 15951747]

Butcher RL, Fugo NW, Collins WE. Semicircadian rhythm in plasma levels of prolactin during early gestation in the rat. Endocrinology 1972;90:1125–1127. [PubMed: 5011056]

Daikoku S, Hisano S, Kagotani Y. Neuronal associations in the rat suprachiasmatic nucleus demonstrated by immunoelectron microscopy. J Comp Neurol 1992;325:559–571. [PubMed: 1361497]

Dardente H, Poirel VJ, Klosen P, Pevet P, Masson-Pevet M. Per and neuropeptide expression in the rat suprachiasmatic nuclei: compartmentalization and differential cellular induction by light. Brain Res 2002;958:261–271. [PubMed: 12470861]

de la Iglesia HO, Schwartz WJ. Minireview: timely ovulation: circadian regulation of the female hypothalamo-pituitary-gonadal axis. Endocrinology 2006;147:1148–1153. [PubMed: 16373412]

Dobson FS, Michener GA. Maternal traits and reproduction in Richardson's ground squirrels. Ecology 1995;76:851–862.

Dunlap JC. Molecular bases for circadian clocks. Cell 1999;96:271–290. [PubMed: 9988221]

Edelstein K, Beaule C, D'Abramo R, Amir S. Expression profiles of JunB and c-Fos proteins in the rat circadian system. Brain Res 2000;870:54–65. [PubMed: 10869501]

Freeman ME, Kanyicska B, Lerant A, Nagy G. Prolactin: structure, function, and regulation of secretion. Physiol Rev 2000;80:1523–1631. [PubMed: 11015620]

Gerall AA, Napoli AM, Cooper UC. Daily and hourly estrous running in intact, spayed and estrone implanted rats. Physiol Behav 1973;10:225–229. [PubMed: 4736131]

Gilbert AN, Rosenwasser AM, Adler NT. Timing of parturition and postpartum mating in Norway rats: interaction of an interval timer and a circadian gate. Physiol Behav 1985;34:61–63. [PubMed: 4041051]

Guido ME, de Guido LB, Goguen D, Robertson HA, Rusak B. Daily rhythm of spontaneous immediate-early gene expression in the rat suprachiasmatic nucleus. J Biol Rhythms 1999;14:275–280. [PubMed: 10447307]

Guilding C, Piggins HD. Challenging the omnipotence of the suprachiasmatic timekeeper: are circadian oscillators present throughout the mammalian brain? Eur J Neurosci 2007;25:3195–3216. [PubMed: 17552989]

Hansen S, Sodersten P, Eneroth P, Srebro B, Hole K. A sexually dimorphic rhythm in oestradiol-activated lordosis behaviour in the rat. J Endocrinol 1979;83:267–274. [PubMed: 521741]

Harlan RE, Shivers BD, Moss RL, Shryne JE, Gorski RA. Sexual performance as a function of time of day in male and female rats. Biol Reprod 1980;23:64–71. [PubMed: 7191337]

Hastings MH, Reddy AB, Maywood ES. A clockwork web: circadian timing in brain and periphery, in health and disease. Nat Rev Neurosci 2003;4:649–661. [PubMed: 12894240]

Ibata Y, Tanaka M, Ichitani Y, Takahashi Y, Okamura H. Neuronal interaction between VIP and vasopressin neurones in the rat suprachiasmatic nucleus. Neuroreport 1993;4:128–130. [PubMed: 8453048]

Ibata Y, Tanaka M, Tamada Y, Hayashi S, Kawakami F, Takamatsu T, Hisa Y, Okamura H. The suprachiasmatic nucelus: a circadian oscillator. Neuroscientist 1997;3:215–225.

Jac M, Sumova A, Illnerova H. c-Fos rhythm in subdivisions of the rat suprachiasmatic nucleus under artificial and natural photoperiods. Am J Physiol Regul Integr Comp Physiol 2000;279:2270–2276.

Johnson RF, Morin LP, Moore RY. Retinohypothalamic projections in the hamster and rat demonstrated using cholera toxin. Brain Res 1988;462:301–312. [PubMed: 3191391]

Kimura M, Zhang SQ, Inoue S. Pregnancy-associated sleep changes in the rat. Am J Physiol Regul Integr Comp Physiol 1996;271:1063–1069.

Kittrell EM, Satinoff E. Diurnal rhythms of body temperature, drinking and activity over reproductive cycles. Physiol Behav 1988;42:477–484. [PubMed: 3393610]

Kovacs KJ. Measurement of immediate-early gene activation- c-fos and beyond. J Neuroendocrinol 2008;20:665–672. [PubMed: 18601687]

Kriegsfeld LJ, Leak RK, Yackulic CB, LeSauter J, Silver R. Organization of suprachiasmatic nucleus projections in Syrian hamsters (*Mesocricetus auratus*): an anterograde and retrograde analysis. J Comp Neurol 2004;468:361–379. [PubMed: 14681931]

Leak RK, Moore RY. Topographic organization of suprachiasmatic nucleus projection neurons. J Comp Neurol 2001;433:312–334. [PubMed: 11298358]

Lee Y, Arbogast LA, Voogt JL. Semicircadian rhythms of c-Fos expression in several hypothalamic areas during pregnancy in the rat: relationship to prolactin secretion. Neuroendocrinology 1998;67:83–93. [PubMed: 9508038]

Levine JD, Weiss ML, Rosenwasser AM, Miselis RR. Retinohypothalamic tract in the female albino rat: a study using horseradish peroxidase conjugated to cholera toxin. J Comp Neurol 1991;306:344–360. [PubMed: 1711060]

Lu J, Zhang YH, Chou TC, Gaus SE, Elmquist JK, Shiromani P, Saper CB. Contrasting effects of ibotenate lesions of the paraventricular nucleus and subparaventricular zone on sleep-wake cycle and temperature regulation. J Neurosci 2001;21:4864–4874. [PubMed: 11425913]

Mahoney MM, Smale L. A daily rhythm in mating behavior in a diurnal murid rodent Arvicanthis niloticus. Horm Behav 2005;47:8–13. [PubMed: 15579260]

Moore-Ede, MC.; Sulzman, FM.; Fuller, CA. The clocks that time us: physiology of the circadian timing system. Cambridge: Harvard University Press; 1982.

Moore RY, Eichler VB. Loss of a circadian adrenal corticosterone rhythm following suprachiasmatic lesions in the rat. Brain Res 1972;42:201–206. [PubMed: 5047187]

Moore RY, Lenn NJ. A retinohypothalamic projection in the rat. J Comp Neurol 1972;146:1–14. [PubMed: 4116104]

Moore RY, Speh JC. GABA is the principal neurotransmitter of the circadian system. Neurosci Lett 1993;150:112–116. [PubMed: 8097023]

Moore RY, Speh JC, Leak RK. Suprachiasmatic nucleus organization. Cell Tissue Res 2002;309:89–98. [PubMed: 12111539]

Morin LP. SCN organization reconsidered. J Biol Rhythms 2007;22:3–13. [PubMed: 17229920]

Morin LP, Goodless-Sanchez N, Smale L, Moore RY. Projections of the suprachiasmatic nuclei, subparaventricular zone and retrochiasmatic area in the golden hamster. Neuroscience 1994;61:391–410. [PubMed: 7526267]

Perrin JS, Segall LA, Harbour VL, Woodside B, Amir S. The expression of the clock protein PER2 in the limbic forebrain is modulated by the estrous cycle. Proc Natl Acad Sci USA 2006;103:5591–5596. [PubMed: 16554373]

Peterfi Z, Churchill L, Hajdu I, Obal F Jr, Krueger JM, Parducz A. Fos-immunoreactivity in the hypothalamus: dependency on the diurnal rhythm, sleep, gender, and estrogen. Neuroscience 2004;124:695–707. [PubMed: 14980739]

Ralph MR, Foster RG, Davis FC, Menaker M. Transplanted suprachiasmatic nucleus determines circadian period. Science 1990;247:975–978. [PubMed: 2305266]

Ramanathan C, Nunez AA, Smale L. Daily rhythms in PER1 within and beyond the suprachiasmatic nucleus of female grass rats (*Arvicanthis niloticus*). Neuroscience 2008;156:48–58. [PubMed: 18692118]

Refinetti R. Phase relationship of the body temperature and locomotor activity rhythms in free-running and entrained rats. Biol Rhythm Res 1997;28:19–24.

Refinetti R. Relationship between the daily rhythms of locomotor activity and body temperature in eight mammalian species. Am J Physiol Regul Integr Comp Physiol 1999;277:1493–1500.

Reppert SM, Weaver DR. Coordination of circadian timing in mammals. Nature 2002;418:935–941. [PubMed: 12198538]

Romijn HJ, Sluiter AA, Wortel J, Van Uum JF, Buijs RM. Immunocytochemical evidence for a diurnal rhythm of neurons showing colocalization of VIP with GRP in the rat suprachiasmatic nucleus. J Comp Neurol 1998;391:397–405. [PubMed: 9492207]

Rosenwasser AM, Hollander SJ, Adler NT. Effects of pregnancy and parturition on free-running circadian activity rhythms in the rat. Chronobiol Int 1987;4:183–187. [PubMed: 3508739]

Rusak B. The role of the suprachiasmatic nuclei in the generation of circadian rhythms in the golden hamster, Mesocricetus auratus. J Comp Physiol A 1977;118:145–164.

Rusak B, Robertson HA, Wisden W, Hunt SP. Light pulses that shift rhythms induce gene expression in the suprachiasmatic nucleus. Science 1990;248:1237–1240. [PubMed: 2112267]

Saper CB, Lu J, Chou TC, Gooley J. The hypothalamic integrator for circadian rhythms. Trends Neurosci 2005;28:152–157. [PubMed: 15749169]

Schwartz MD, Nunez AA, Smale L. Differences in the suprachiasmatic nucleus and lower subparaventricular zone of diurnal and nocturnal rodents. Neuroscience 2004;127:13–23. [PubMed: 15219664]

Schwartz MD, Nunez AA, Smale L. Rhythmic cFos expression in the ventral subparaventricular zone influences general activity rhythms in the Nile grass rat, Arvicanthis niloticus. Chronobiol Int 2009;26:1290–1306. [PubMed: 19916832]

Schwartz WJ, Carpino A Jr, de la Iglesia HO, Baler R, Klein DC, Nakabeppu Y, Aronin N. Differential regulation of fos family genes in the ventrolateral and dorsomedial subdivisions of the rat suprachiasmatic nucleus. Neuroscience 2000;98:535–547. [PubMed: 10869847]

Schwartz WJ, Takeuchi J, Shannon W, Davis EM, Aronin N. Temporal regulation of light-induced Fos and Fos-like protein expression in the ventrolateral subdivision of the rat suprachiasmatic nucleus. Neuroscience 1994;58:573–583. [PubMed: 8170538]

Stephan FK, Zucker I. Circadian rhythms in drinking behavior and locomotor activity of rats are eliminated by hypothalamic lesions. Proc Natl Acad Sci USA 1972;69:1583–1586. [PubMed: 4556464]

Sumova A, Illnerova H. Effect of photic stimuli disturbing overt circadian rhythms on the dorsomedial and ventrolateral SCN rhythmicity. Brain Res 2005;1048:161–169. [PubMed: 15913573]

Sumova A, Travnickova Z, Illnerova H. Spontaneous c-Fos rhythm in the rat suprachiasmatic nucleus: location and effect of photoperiod. Am J Physiol Regul Integr Comp Physiol 2000;279:2262–2269.

Thomas EM, Armstrong SM. Effect of ovariectomy and estradiol on unity of female rat circadian rhythms. Am J Physiol Regul Integr Comp Physiol 1989;257:1241–1250.

Watts, AG. The efferent projections of the suprachiasmatic nucleus: anatomical insights into the control of circadian rhythms. In: Klein, DC.; Moore, RY.; Reppert, SM., editors. Suprachiasmatic Nucleus: The Mind's Clock. New York: Oxford University Press; 1991. p. 77-106.

Watts AG, Swanson LW. Efferent projections of the suprachiasmatic nucleus: II. Studies using retrograde transport of fluorescent dyes and simultaneous peptide immunohistochemistry in the rat. J Comp Neurol 1987;258:230–252. [PubMed: 2438309]

Watts AG, Swanson LW, Sanchez-Watts G. Efferent projections of the suprachiasmatic nucleus: I. Studies using anterograde transport of Phaseolus vulgaris leucoagglutinin in the rat. J Comp Neurol 1987;258:204–229. [PubMed: 3294923]

Weinert D. Ontogenetic development of the mammalian circadian system. Chronobiol Int 2005;22:179–205. [PubMed: 16021838]

Abbreviations

3v	third ventricle
ABC	avidin-biotin peroxidase complex
ACTH	adrenal corticotropin hormone
ANOVA	analysis of variance
AVP	arginine vasopressin
CT	circadian time
DAB	diaminobenzidine
DD	constant darkness
dm	dorsomedial
ER-*β*	estrogen-receptor beta
Fos	protein product of the *cfos* gene
GRP	gastrin-releasing peptide
ir	immunoreactivity

LD	light/dark
LSD	least significant difference
NGS	normal goat serum
NHS	normal horse serum
NREMS	non-rapid eye movement sleep
ocx	optic chiasm
OVX	ovariectomized
PBS	0.01 M phosphate-buffered saline
Per	period
Per2	protein product of the *per2* gene
REMS	rapid eye movement sleep
SCN	suprachiasmatic nucleus
SPZ	subparaventricular zone
TH	tyrosine hydroxylase
TX	Triton-X 100
VIP	vasoactive intestinal peptide
vl	ventrolateral
vSPZ	ventral subparaventricular zone
ZT	zeitgeber time

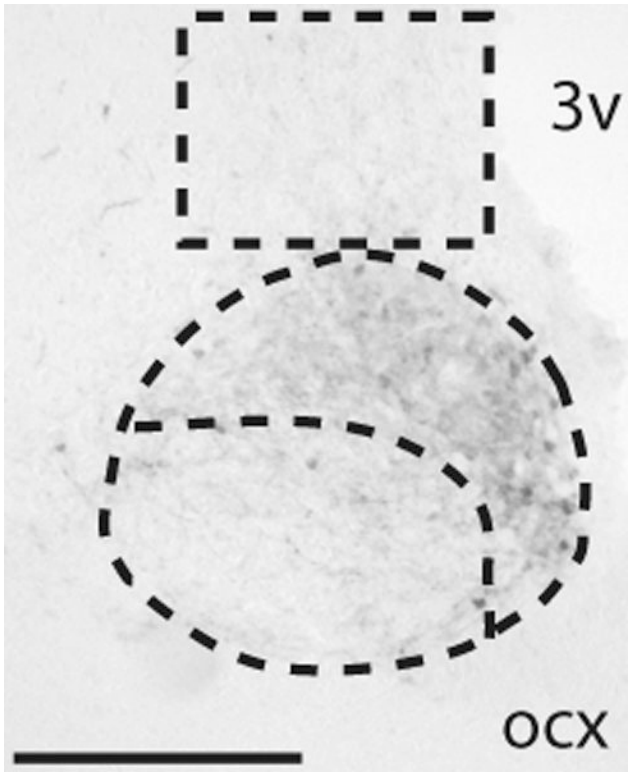

Fig. 1.
Photomicrograph of the SCN and vSPZ of a female lab rat stained for AVP-immunoreactivity (-ir). The middle SCN core and AVP-rich SCN shell are outlined, and the sampling box used for vSPZ counts is placed above the SCN. ocx, optic chiasm; 3v, third ventricle. Scale bar = 200 μm.

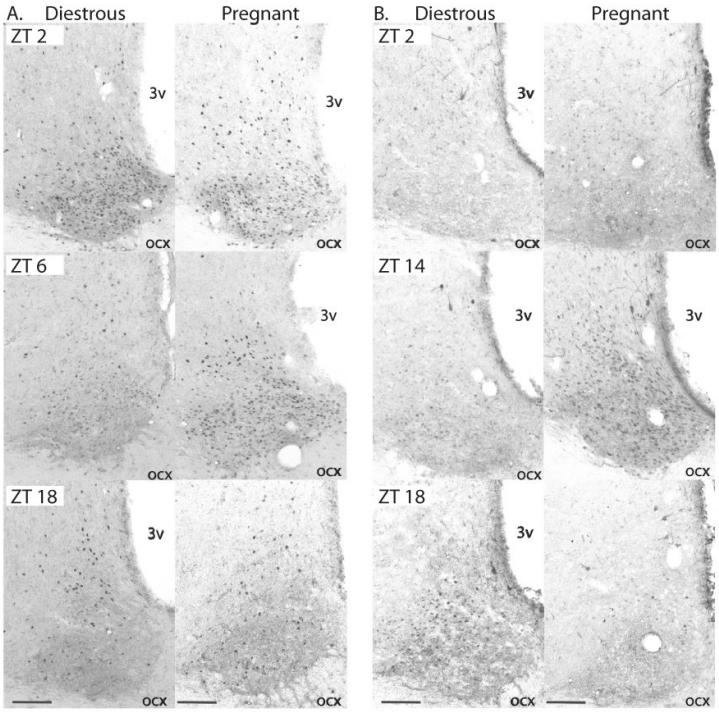

Fig. 2.

Representative photomicrographs of protein expression of Fos at ZT 2, 6, and 18 (A) and Per2 at ZT 2, 14, and 18 (B) in the middle SCN and vSPZ of diestrous (left) and pregnant rats (right) kept in a 12:12 LD cycle. Per2 is only expressed in the cell nucleus. Larger cells in (B) that are stained in the cytoplasm are TH-ir cells and are primarily located around the vSPZ and 3v (see METHODS). ocx, optic chiasm; 3v, third ventricle. Scale bars = 100 μm.

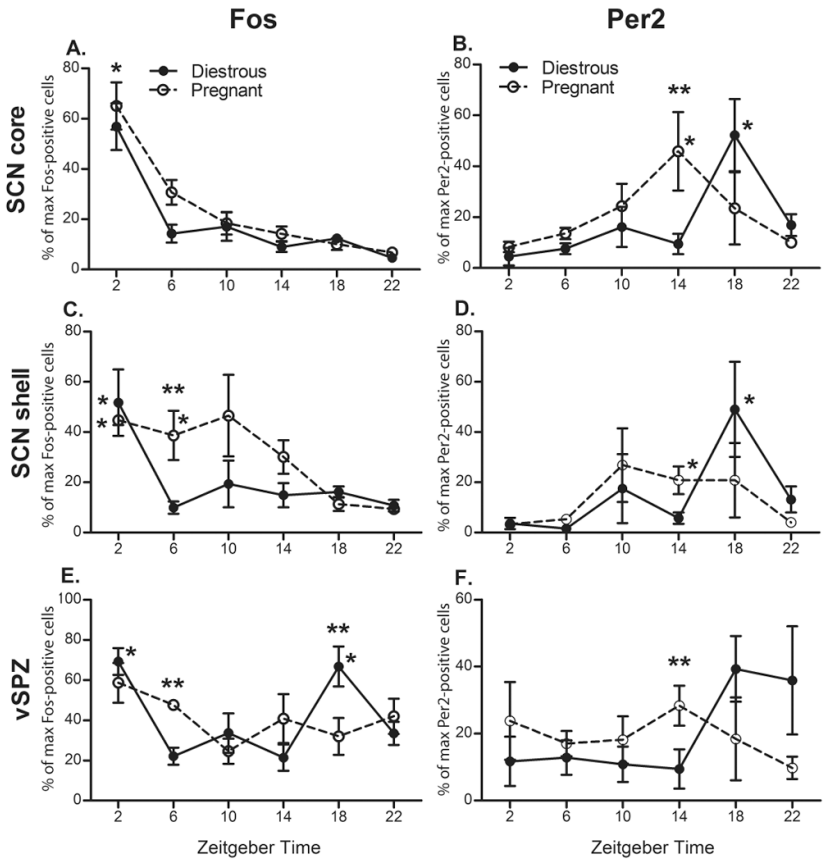

Fig. 3.

Expression of Fos (left column) and Per2 (right column) in the SCN core (A,B), SCN shell (C,D), and vSPZ (E,F) of diestrous and pregnant rats kept in a 12:12 LD cycle. Expression is measured as the percentage of the maximum individual value for each protein in each region. *indicates a time point where expression is significantly elevated relative to at least two other time points within the same reproductive state ($P<0.05$, post-hoc LSD (A,B,E,F) or Mann-Whitney U (C,D) tests), and **indicates a time point at which expression significantly differs between reproductive states ($P<0.05$, post-hoc LSD (A,B,E,F), or $P<0.017$, Mann-Whitney U (C) tests).

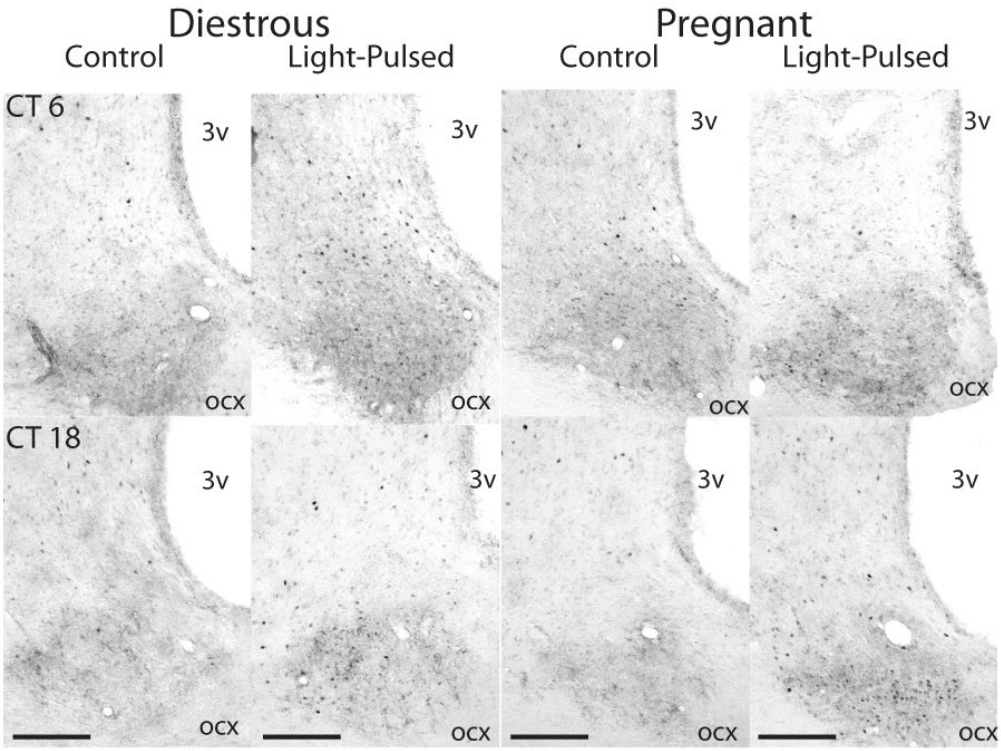

Fig. 4.

Representative photomicrographs of protein expression of Fos in the middle SCN and vSPZ of control and light-pulsed diestrous (left) and pregnant rats (right) at CT 6 (top row) and CT 18 (bottom row). ocx, optic chiasm; 3v, third ventricle. Scale bars = 100 μm.

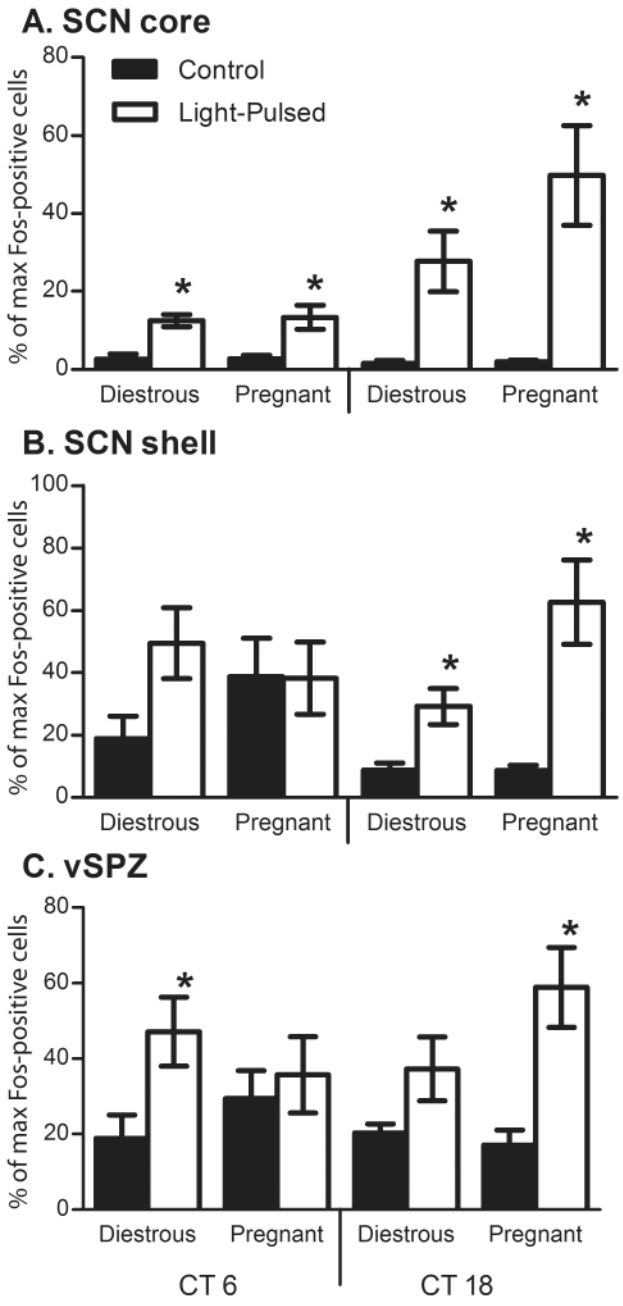

Fig. 5.

Expression of Fos in the SCN core (A), SCN shell (B), and vSPZ (C) of control and light-pulsed diestrous and pregnant rats kept in DD for two days. Expression is measured as the percentage of the maximum individual Fos-positive cell count within the region of interest. * indicates significantly higher Fos expression in light-pulsed than control females ($P<0.01$, Mann-Whitney U (A,B) tests, or $P<0.05$, post-hoc LSD (C) tests).